

# Analogy between Three-Dimensional Helimagnetic Metals and Two-Dimensional Nonmagnetic Metals: Transport in the Weak-Disorder Regime

T.R. Kirkpatrick<sup>1</sup>, D. Belitz<sup>2,3</sup>, and Ronojoy Saha<sup>2</sup>

<sup>1</sup>*Institute for Physical Science and Technology and Department of Physics,  
University of Maryland, College Park, MD 20742*

<sup>2</sup>*Department of Physics and Institute of Theoretical Science, University of Oregon, Eugene, OR 97403*

<sup>3</sup>*Kavli Institute for Theoretical Physics, University of California, Santa Barbara, CA 93106*

(Dated: April 26, 2019)

We present a quasi-particle model that allows for a simple description of the electronic properties of metallic helimagnets. For weak quenched disorder, we find a leading linear temperature dependence of the electrical conductivity for 3-*d* materials. This is reminiscent of the behavior of nonmagnetic 2-*d* systems, and reflects a general tendency of certain properties of bulk helimagnets to appear effectively 2-*d*. The sign of the effect is opposite to that in nonmagnetic 2-*d* materials. These surprising predictions should be observable in weak helimagnets.

PACS numbers: 75.30.Ds; 75.30.-m; 75.50.-y; 75.25.+z

Helimagnets (e.g., MnSi, or FeGe) are magnetic materials where the magnetization shows ferromagnetic order in any plane perpendicular to a certain axis, but points in different directions depending on the position along that axis, forming a spiral. The metallic helimagnet MnSi is a well-studied material with unusual properties. It shows helical order below a critical temperature  $T_c \approx 30$  K with a helix wavelength  $2\pi/q \approx 180 \text{ \AA}$  [1]. Hydrostatic pressure decreases  $T_c$  until the long-range order [2] disappears at a critical pressure  $p_c \approx 14$  kbar [3]. At higher pressure, there is a phase or region where short-range helical order persists and the electrical resistivity  $\rho$  shows a  $T^{3/2}$  temperature dependence in a range between a few mK and several K [4]. If this were the true asymptotic low- $T$  behavior, it would represent non-Fermi liquid behavior in a bulk material, which would be very remarkable.

The samples used in Ref. 4 have a residual resistivity of about  $0.3 \mu\Omega\text{cm}$ , which corresponds to a rather large elastic mean-free time  $\tau$ . At the experimentally attainable temperatures, this places them in the weak-disorder regime,  $T\tau \gg 1$  [5], where the transport is governed by free-electron motion in between rare scattering events, as opposed to diffusive motion in the opposite limit,  $T\tau \ll 1$ . The weak-disorder regime has been investigated by Zala et al. [6] for the case of electrons interacting via a screened Coulomb interaction in non-magnetic 2-*d* metals, where they found a linear  $T$  dependence of the resistivity. (In 3-*d*, the corresponding resistivity correction is of  $O(T^2 \ln T)$  [7].) Although the weak-disorder regime is never the true asymptotic low-temperature regime, it thus can display very unusual behavior. Furthermore, depending on the impurity concentration, it can represent the low- $T$  asymptotics for practical purposes.

In a helimagnet, massless fluctuations of the helix (helimagnons) that couple to the electrical conductivity are an obvious possible source for unusual transport behavior, and it is natural to first study their effects in the ordered phase, before trying to understand their potential rami-

fications more generally [8]. It was recently shown that helimagnons do indeed lead to a non-analytic temperature dependence of the resistivity in the ordered phase [9]. However, for the most interesting observables in a clean system these effects provide *corrections* to the usual Fermi-liquid behavior: the leading helimagnon contribution to the resistivity has a  $T^{5/2}$  behavior, and the specific heat goes as  $T^2$ , although the single-particle relaxation rate goes as  $T^{3/2}$ .

In this Rapid Communication we investigate the resistivity of 3-*d* helimagnets in the weak-disorder regime (which is defined slightly differently than in the Coulomb case, see below). We show that the leading temperature correction  $\delta\rho(T)$  to the resistivity is proportional to  $T$  due to scattering by helimagnons. Remarkably, this is much stronger than either the  $T^{5/2}$  clean helimagnon contribution or the  $T^2$  Fermi-liquid contribution, and it is reminiscent of the behavior of 2-*d* nonmagnetic metals. In contrast to the latter, however, the sign of the  $T$ -dependence is antilocalizing: there is a  $T$ -independent part that decreases the resistivity, and the  $T$ -dependent part is  $\delta\rho \propto +T\tau$ .

Transport theory for helimagnets is rather complicated, even in the clean case, if the Kubo formula is evaluated using the usual plane-wave basis. In this basis, the electronic Green function is not diagonal in either wave vector space or spin space, which makes for very cumbersome calculations [9]. Including impurity scattering in this formalism would be hard. However, several features of this theory, which we quote below, suggest a much simpler effective description. The poles of the electronic Green function, or quasi-particle (QP) energies, are given by

$$\omega_{1,2}(\mathbf{k}) = \frac{1}{2} \left( \xi_{\mathbf{k}} + \xi_{\mathbf{k}+\mathbf{q}} \pm \sqrt{(\xi_{\mathbf{k}} - \xi_{\mathbf{k}+\mathbf{q}})^2 + 4\lambda^2} \right). \quad (1)$$

Here  $\xi_{\mathbf{k}} = \epsilon_{\mathbf{k}} - \epsilon_F$ , with  $\epsilon_{\mathbf{k}}$  the electronic energy-momentum relation and  $\epsilon_F$  the chemical potential. For a

cubic crystal, such as MnSi,

$$\epsilon_{\mathbf{k}} = \frac{\mathbf{k}^2}{2m_e} + \frac{\nu}{2m_e k_F^2} (k_x^2 k_y^2 + k_y^2 k_z^2 + k_z^2 k_x^2) + O(k^6), \quad (2)$$

with  $m_e$  the effective electron mass, and  $\nu = O(1)$  a dimensionless measure of deviations from nearly free electrons. We choose units such that  $\hbar = k_B = e = 1$ .  $\mathbf{q} = (0, 0, q)$  is the helix pitch vector, which we choose to point in the  $z$ -direction, and  $\lambda$  is the Stoner splitting. The two signs of the square root represent the two Stoner bands, and for  $\mathbf{q} = 0$  one recovers the usual ferromagnetic result in Stoner approximation. Excitations between the two Stoner bands will be gapped by  $\lambda$ , and we can thus restrict ourselves to a single band by considering spinless QPs with a resonance frequency  $\omega_1(\mathbf{k})$ .

For the electronic QP Green function one thus expects

$$G_0(p) = 1/(i\omega_n - \omega_1(\mathbf{p})), \quad (3)$$

where  $p = (\mathbf{p}, i\omega_n)$  with  $\omega_n$  a fermionic Matsubara frequency [10]. We have shown that such a QP Green function can indeed be derived from a canonical transformation to suitable fermionic degrees of freedom  $\eta(p)$  [11]. The soft, or massless, helical degrees of freedom, the helimagnons, are fluctuations of a generalized helical phase  $\phi$  with a frequency

$$\omega_0(\mathbf{p}) = \sqrt{c_z p_z^2 + c_\perp p_\perp^4}. \quad (4a)$$

Here  $p_z$  and  $p_\perp$  are the longitudinal and transverse components, respectively, of the wave vector with respect to the pitch wave vector  $\mathbf{q}$ , and the elastic constants  $c_z$  and  $c_\perp$  are given by

$$c_z = \gamma_z \lambda^2 q^2 / k_F^4, \quad c_\perp = \gamma_\perp \lambda^2 / k_F^4. \quad (4b)$$

$\gamma_z$  and  $\gamma_\perp$  are model-dependent numbers. For the model considered in Ref. [9], their values are  $\gamma_z = 1/36$  and  $\gamma_\perp = 1/96$ . Equation (4a) is valid for  $|\mathbf{p}| < q$ . Notice that the helimagnon dispersion relation is anisotropic: it is ferromagnet-like in the longitudinal direction, but antiferromagnet-like in the transverse direction. The helimagnon susceptibility is given by

$$\chi(k) = \langle \phi(k) \phi(-k) \rangle = \frac{1}{2N_F} \frac{q^2 / 3k_F^2}{\omega_0^2(\mathbf{k}) - (i\Omega_n)^2}, \quad (5)$$

with  $\Omega_n$  a bosonic Matsubara frequency,  $k = (\mathbf{k}, i\Omega_n)$ , and  $N_F$  the density of states at the Fermi level. We see that frequency or temperature scale with the soft wave vector  $\mathbf{k}$  as  $T \sim k_z \sim k_\perp^2$ .

Since  $\phi$  is a phase, only the gradient of  $\phi$  is of physical significance and will couple to the QPs. Furthermore, the results of Ref. 9 show that the leading coupling is not to the QP density, but rather to the  $z$ - $\perp$  components of the QP stress. Upon integrating out  $\phi$ , one thus expects an effective potential for the interaction of QPs by means of

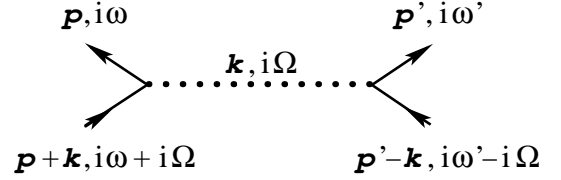


FIG. 1: Effective interaction between QPs (solid lines) by exchange of a helimagnon (dotted line).

exchange of helimagnons that is given pictorially in Fig. 1, and analytically by

$$V_{\text{eff}} = -\lambda^2 (q^2 / 8m_e^2) \chi(k) \gamma(\mathbf{k}, \mathbf{p}) \gamma(\mathbf{k}, \mathbf{p}'), \quad (6a)$$

with a vertex function

$$\gamma(\mathbf{k}, \mathbf{p}) = \nu p_z (\mathbf{p}_\perp \cdot \mathbf{k}_\perp) / \lambda k_F^2. \quad (6b)$$

Finally, we expect static impurities or quenched disorder to couple to the QP density. Putting everything together, we now have the following effective action:

$$S = S_0 + S_{\text{int}} + S_{\text{dis}}, \quad (7a)$$

where

$$S_0 = (T/V) \sum_p \bar{\eta}(p) [i\omega_n - \omega_1(p)] \eta(p) \quad (7b)$$

describes free QPs,

$$S_{\text{int}} = \frac{-T}{V} \sum_k \frac{1}{V^2} \sum_{\mathbf{p}, \mathbf{p}'} V_{\text{eff}}(k; \mathbf{p}, \mathbf{p}') T \sum_{i\omega} \bar{\eta}(\mathbf{p}, i\omega) \times \eta(\mathbf{p} + \mathbf{k}, i\omega + i\Omega) \bar{\eta}(\mathbf{p}', i\omega) \eta(\mathbf{p}' - \mathbf{k}, i\omega - i\Omega) \quad (7c)$$

describes the effective QP interaction via the exchange of a helimagnon, and

$$S_{\text{dis}} = (-1/V^2) \sum_{\mathbf{k}, \mathbf{p}} u(\mathbf{k} - \mathbf{p}) T \sum_{i\omega} \bar{\eta}(\mathbf{k}, i\omega) \eta(\mathbf{p}, i\omega) \quad (7d)$$

describes the quenched disorder. Here  $u$  is a delta-correlated point-like random potential with a Gaussian distribution whose second moment is given by  $1/2\pi N_F \tau$ .

The Eqs. (7) represent an effective model for QPs interacting via a dynamical potential that allows for an evaluation of the Kubo formula in complete analogy to electrons interacting via a dynamically screened Coulomb interaction. The only unusual aspects are, (1) the coupling to the QP stress rather than the density, and (2) the anisotropic nature of the exchanged excitations. The former is embodied in the vertex functions  $\gamma$  in Eqs. (6) and easy to handle technically, but has important physical consequences. The latter makes the bulk system behave in some respects like a 2- $d$  system. We have derived this effective model from the one studied in Ref. 9 by

means of a canonical transformation [11]; the above considerations represent just plausibility arguments.

Transport theory now proceeds in analogy to the Coulomb problem. In order to calculate the static electrical conductivity tensor  $\sigma_{ij}$  we evaluate the Kubo formula

$$\sigma_{ij} = -\lim_{\Omega \rightarrow 0} \text{Re} \frac{i}{i\Omega_n} \int_0^{1/T} d\tau e^{i\Omega_n \tau} \left\langle T_\tau \hat{j}_i(\mathbf{k}, \tau) \times \hat{j}_j(\mathbf{k}, \tau = 0) \right\rangle \Big|_{i\Omega_n \rightarrow \Omega + i0, \mathbf{k}=0}, \quad (8)$$

with  $\hat{j}(\mathbf{k}, \tau)$  the current operator in imaginary-time representation and  $T_\tau$  the imaginary-time ordering operator. The tensor  $\sigma_{ij}$  is diagonal and has two independent elements,  $\sigma_L \equiv \sigma_{zz}$  and  $\sigma_\perp \equiv \sigma_{xx} = \sigma_{yy}$ .

In the clean limit,  $\tau \rightarrow \infty$ , we reproduce the results of Ref. 9: an infinite ladder resummation of both the self-energy and vertex-correction contributions to the conductivity shows that the leading low- $T$  terms cancel between the two sets of diagrams. The transport relaxation rate, and hence the resistivity, shows a  $T^{5/2}$  behavior, whereas the single-particle relaxation rate goes as  $T^{3/2}$ .

In the weak-disorder limit, it is convenient to include the disorder in the Green function in the Born approximation, i.e., to use a Green function

$$G(p) = 1/(i\omega_n - \omega_1(\mathbf{p}) + i \text{sgn}(\omega_n)/2\tau) \quad (9)$$

instead of Eq. (3). The diagrams that contribute to the correction to the conductivity to leading order in the disorder in the weak-disorder limit are shown in Fig. 2; they are the same as in Ref. 6.

Diagrams (i) and (ii) also contribute in the clean limit, where their respective ladder resummations must

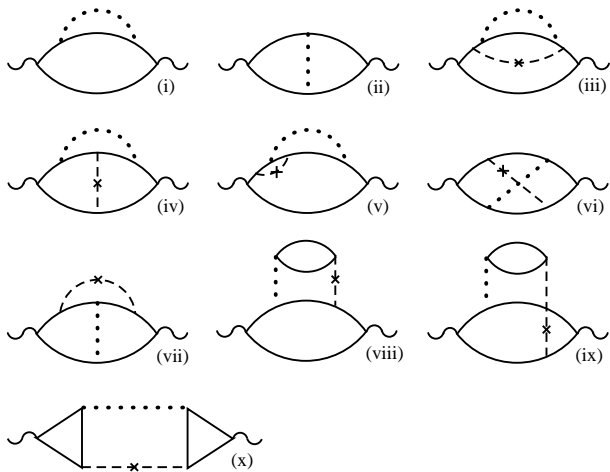


FIG. 2: Leading contributions to the conductivity in the weak-disorder limit. Solid lines represent the Green function given by Eq. (9), dotted lines represent the effective potential, Eqs. (6), and dashed lines represent the impurity factor  $1/2\pi N_F \tau$ . Obvious symmetric counterparts of all diagrams except (ii) are not shown. See the text for additional information.

be taken into account. In the presence of disorder, their leading terms are proportional to  $\tau^2 T^{3/2}$ . (This is the result of adding the clean single-particle rate, which is proportional to  $T^{3/2}$ , to  $1/\tau$  according to Matthiessen's rule, and expanding.) These terms cancel between diagrams (i) and (ii), as they must according to Ref. 9. The calculation shows that the small parameter for the disorder expansion is  $\epsilon = 1/\sqrt{\tau^2 T \epsilon_F^2/\lambda}$ . This is different from the Coulomb case, where the small parameter is  $1/\tau T$  [6]. Consequently, the next-leading terms are of order  $\tau T$ . These also cancel between the two diagrams.

For the remaining diagrams it suffices to calculate their leading behavior, and they can be classified with respect to their momentum structure. They each contain six Green functions that factorize into two correlation functions formed by  $n$  and  $6-n$  Green functions, respectively, with  $n = 3$  or  $n = 4$ . Power counting shows that the  $(4, 2)$  partitions are smaller than the  $(3, 3)$  partitions by a factor of  $(q/k_F)^2$ . Dropping the former leaves us with diagrams (iii), (iv), (vi). Diagram (x) also is a  $(3, 3)$  partition, but its leading contribution vanishes due to reality requirements. Furthermore, power counting reveals that for  $\sigma_\perp$ , only diagram (iii) is of  $O(\tau T)$ , whereas for  $\sigma_L$  one needs to consider diagrams (iv) and (vi) as well.

We thus conclude that the leading contributions to both the longitudinal and the transverse conductivity corrections are of  $O(\tau T)$ . We find

$$\delta\sigma_L = 3\delta\sigma_\perp = -\sigma_0 \frac{\pi\nu^2}{192\sqrt{\gamma_z\gamma_\perp}} \left(\frac{\epsilon_F}{\lambda}\right)^2 \left(\frac{q}{k_F}\right)^3 \frac{T}{\epsilon_F}, \quad (10)$$

with  $\sigma_0 = (2k_F/3\pi^2)\epsilon_F\tau$  the Drude conductivity. In writing this result we have dropped a  $T$ -independent UV-cutoff dependent contribution to  $\delta\sigma$  whose sign is opposite that of the  $T$ -dependent contribution.

We now discuss this result. First, notice the sign of the result.  $\delta\sigma$  increases with decreasing  $T$ , which means the effect is antilocalizing. This is in contrast to the Coulomb case, where the sign is localizing. The sign is the same for both the self-energy diagram (iii), and the vertex correction diagrams (iv) and (vi). In the former, it is a result of the angular dependence of the effective interaction, Eq. (6b), which in turn is a result of the stress coupling, and which suppresses backscattering in diagram (iii). For a density coupling, diagram (iii) would be localizing.

Second, we discuss the range of validity of our result. The weak-disorder temperature regime is bounded below by the requirement that the expansion parameter  $\epsilon$  be small, i.e.,  $T\tau^2\epsilon_F^2/\lambda \gg 1$ . This defines a temperature scale  $T^* = \lambda/(\epsilon_F\tau)^2$ . It is bounded above by the weak-disorder correction to the relaxation rate crossing over to either the clean-limit rate  $1/\tau_{\text{clean}} \propto T^{5/2}$  [9], or to the Fermi-liquid rate  $1/\tau_{\text{FL}} \approx T^2/\epsilon_F$ . For the former, we have a crossover temperature  $T_{1-5/2} = \lambda/(\epsilon_F\tau)^{2/3}$ , for the latter,  $T_{1-2} = (1/\tau)(q/k_F)^3(\epsilon_F/\lambda)^2$ . The weak-

disorder rate thus yields the dominant  $T$  dependence of the resistivity in the regime

$$T^* \ll T \ll \text{Min}(T_{1-2}, T_{1-5/2}), \quad (11)$$

and  $T_{1-2}/T_{1-5/2} = (q/k_F)^3(\epsilon_F/\lambda)^3/(\epsilon_F\tau)^{1/3}$ . If  $\lambda \lesssim \epsilon_F$ , then  $T_{1-2} \ll T_{1-5/2}$ . In a weak helimagnet, where  $\lambda/\epsilon_F$  might be as small as  $q/k_F$ , we still have  $T_{1-2} < T_{1-5/2}$  on account of the factor  $1/(\epsilon_F\tau)^{1/3}$ . For realistic parameter values, the weak-disorder regime will thus be

$$T^* \ll T \ll T_{1-2} = T^* (\epsilon_F\tau)(q/k_F)^3(\epsilon_F/\lambda)^3. \quad (12)$$

The upper limit depends strongly on  $\epsilon_F/\lambda$ , which is often not well known. For weak helimagnets, with  $\lambda \ll \epsilon_F$ , it is possible to have  $T_{1-2} \gg T^*$  by virtue of  $\epsilon_F\tau \gg 1$ . For larger values of  $\lambda$  the weak-disorder correction may never dominate unless the system is extremely clean. In that case, one will have to subtract the Fermi-liquid  $T^2$  behavior in order to observe the weak-disorder contribution. For MnSi, with  $\epsilon_F \approx 23,000$  K and  $\epsilon_F\tau \approx 1,000$  for the samples of Ref. 4, one has  $T^* \approx 10$  mK.  $q/k_F \approx 0.02$ , but the value of  $\lambda$  is not well known. For the upper and lower limits used in Ref. 9, namely,  $\lambda = \epsilon_F/2$  and  $\lambda = 540$  K, respectively, we find  $T_{1-2} \approx 0.06 T^*$  and  $T_{1-2} \approx 500 T^*$ , which again underscores the strong dependence on  $\epsilon_F/\lambda$ . Generally speaking, weak helimagnets are the best candidates for observing the weak-disorder transport regime.

Third, the anisotropic helimagnon dispersion relation, Eq. (4a), leads to a 3- $d$  helimagnetic system being qualitatively similar to a 2- $d$  one with just a Coulomb interaction. The components of the soft wave vector  $\mathbf{k}$  scale as  $k_z \sim k_\perp^2 \sim T$ . With  $f(\mathbf{k})$  a generic function, the relevant integrals that determine observables are of the form

$$\int dk_z \int d\mathbf{k}_\perp k_\perp^2 \delta(\Omega^2 - k_z^2 - \mathbf{k}_\perp^4) f(k_z, \mathbf{k}_\perp) \propto \int d\mathbf{k}_\perp k_\perp^2 \frac{\Theta(\Omega^2 - \mathbf{k}_\perp^4)}{\sqrt{\Omega^2 - \mathbf{k}_\perp^4}} f(k_z = 0, \mathbf{k}_\perp),$$

and the dependence of  $f$  on  $k_z$  can be dropped since it does not contribute to the leading temperature scaling. The prefactor of the  $\mathbf{k}$  dependence of  $f$  is of  $O(1)$  in a scaling sense. As a result, the 3- $d$   $\mathbf{k}$ -integral behaves effectively like the integral in the 2- $d$  Coulomb case [12]. In addition to the conductivity, these considerations apply to weak-disorder corrections to the spin susceptibility, and to the specific heat [11].

Finally, we point out a generic feature relevant for the explanation of the  $T^{3/2}$  dependence of the resistivity observed in the disordered phase of MnSi. The prefactor of  $T/\epsilon_F$  in  $\delta\sigma_L/\sigma_0$ , Eq. (10), is very small. Assuming  $\nu = 1$  and the above parameter values for MnSi, it is about  $3 \times 10^{-5}$  for  $\lambda = \epsilon_F/2$ , and about  $10^{-2}$  for  $\lambda = 540$  K. The small prefactor reflects the long wavelength of the helix on a microscopic scale. The prefactor of the  $T^{5/2}$  behavior in the clean limit is also small, for the same

reason. By contrast, the prefactor of the experimentally observed  $(T/\epsilon_F)^{3/2}$  behavior of the resistivity in the disordered phase is of  $O(10^6)$ . Therefore, the processes causing the  $T^{3/2}$  behavior in MnSi must occur on short length scales, and are unlikely to be related to the helical order.

In conclusion, we predict that in the ordered phase of metallic helimagnets, at low temperatures in the weak-disorder regime, the leading temperature correction to the Drude conductivity is proportional to  $T\tau$ , and the size of this effect depends on the direction of the current. This small but very remarkable effect should be most easily observable in weak helimagnets.

This research was supported by the National Science Foundation under Grant Nos. DMR-05-30314, DMR-05-29966, and PHY05-51164.

- 
- [1] Y. Ishikawa, K. Tajima, D. Bloch, and M. Roth, *Solid State Commun.* **19**, 525 (1976).
  - [2] Strictly speaking, there never is any true long-range helical order at any nonzero temperature due to strong fluctuations of the helix, see Ref. 13. However, this is a weak effect that we will neglect for our present purposes.
  - [3] C. Pfleiderer, G. J. McMullan, S. R. Julian, and G. G. Lonzarich, *Phys. Rev. B* **55**, 8330 (1997).
  - [4] C. Pfleiderer, S. R. Julian, and G. G. Lonzarich, *Nature* **414**, 427 (2001).
  - [5] This regime is also referred to as the intermediate-temperature regime, or the ballistic regime. Here we refer to it as the weak-disorder regime, in order to avoid a connotation of ballistic transport in mesoscopic systems.
  - [6] G. Zala, B. N. Narozhny, and I. L. Aleiner, *Phys. Rev. B* **64**, 214204 (2001).
  - [7] A. Sergeev, M. Y. Reizer, and V. Mitin, *Phys. Rev. B* **69**, 075310 (2005).
  - [8] In a rotationally invariant model, effects of helical fluctuations will be strongest in the ordered phase. In a crystal, crystal-field effects will pin the helix, which makes the helical excitations massive. Such pinning is expected to disappear in a phase where the helical order is destroyed, but still persists on some length scales. A rotationally invariant model of the ordered phase may therefore provide a reasonable description of the high-pressure phase, and insight into the transport properties of the ordered phase might give clues about the origin of the observed  $T^{3/2}$  behavior.
  - [9] D. Belitz, T. R. Kirkpatrick, and A. Rosch, *Phys. Rev. B* **74**, 024409 (2006).
  - [10] It is not obvious that it is possible to find a quasi-particle description where the Green function is diagonal in momentum space. However, the canonical transformation mentioned in the text shows that it is.
  - [11] T. R. Kirkpatrick, D. Belitz, and Ronojoy Saha, unpublished results.
  - [12] It is important for this argument that there is no qualitative difference between a stress coupling and a density coupling. This is true in the weak-disorder limit but not, for instance, in the diffusive limit.
  - [13] T. R. Kirkpatrick and D. Belitz, *Phys. Rev. Lett.* **97**, 267205 (2006).